

A Current Controller Design for Current Source Inverter-fed PMSM Drive System

Hak-Jun Lee, Sungho Jung, and Seung-Ki Sul

Dept. Electrical Engineering, Seoul National University, Daehak dong, Gwanak-gu, Seoul, Korea

Abstract— A current source inverter (CSI) requires a capacitor filter for the commutation of switching device as well as attenuating switching harmonics. This paper presents the current controller design of CSI-fed PMSM (Permanent Magnet Synchronous Machine) drive system in order to attenuate resonance due to the LC filter. Basically, the CSI-fed drive system is modeled as a 2nd order system. Hence a multi-loop current controller design using a pole/zero cancellation method is proposed with a transfer function matrix. To compensate the cross-coupling term, two types of controller are implemented using different decoupling method. Additionally, active damping methods are proposed to enhance the stability of the system. To evaluate the effectiveness of the proposed current controller, computer simulation and experiment have been performed and the results are discussed.

Index Terms—Current controller, Current source inverter, PMSM

I. INTRODUCTION

Because of high efficiency, high power density and low maintenance costs, the Permanent Magnet Synchronous Machine (PMSM) has been the most attractive electric machine in many applications, especially in wind turbine generator system. Besides, traditionally, the CSI (Current Source Inverter) had been used for the high power drives due to its ruggedness to over current / short circuit and low dv/dt voltage over the stator windings [1][2]. Recently, because of inherent advantages of CSI and PMSM, the efforts have been increased to drive the PMSM with CSI in high power such as a wind power generation and hybrid vehicles [3][4].

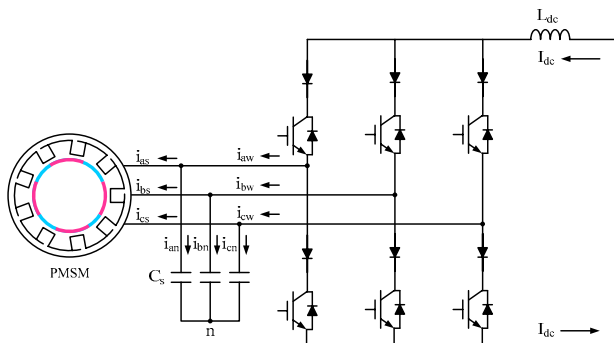


Fig. 1. Block diagram of CSI-fed a PMSM

There was a comparative study with consideration on selection of power semiconductors [5]. Because the cost and size of passive components can be reduced as the

switching frequency is increased, in this paper, the IGBT based CSI is adopted to increase the switching frequency more than 1 kHz even in MW drive system [5]. The CSI-fed PMSM can be depicted as shown in Fig. 1. The three phase filter capacitor C_s is required for commutation of switching devices and filtering out the current harmonics to PMSM. Due to this filter capacitor, the CSI-fed drive system has inherent issue with LC resonance. Because a passive damping method with physical resistors incurs excessive energy losses, there were many studies to dampen the LC resonance with active control strategy. In order to reduce the resonance, there were several approaches which are the virtual resistor damping method [6], feed-forward compensation method from LC filter model [7], compensator design method [8], and hybrid type method with virtual resistor and compensator [9]. However, all of these methods have problem with tuning parameters. On the other hand, the multi-loop controller can generally be used to control the output with a higher order plant [10] such as the CSI-fed drive system employing LC filter. There was a study about the multi-loop controller for VSI (Voltage Source Inverter) with LCL filter and CSI with LC filter [10]. In this study, the Proportional and Resonant (PR) controller was used to attenuate the resonance instead of the PI controller in synchronous reference frame. Due to the PR controller, it has inherent problems with steady state error and selection of gains.

In this paper, the multi-loop current controller based on two stages modeling of the CSI-fed PMSM is proposed. As the current controller, simple PI controller is employed and its gains are set in the technical optimum, which cancel the pole of plant by the zero of the controller in synchronous reference frame. With proposed controller the transfer function between the actual stator current to its reference can be designed as 2nd order low pass filter. The gains for the current controller can be easily determined by LC parameters of CSI. Two kinds of decoupling methods are addressed to compensate the coupling term which is incurred by coordinate transformation to the synchronous reference frame. In addition, active damping methods using virtual resistance are also embedded in the controller to avoid the unstable characteristics due to the parameter error and other disturbances such as digital delay.

II. SYSTEM DESCRIPTION

The CSI-fed PMSM in synchronous reference frame can be modeled as (1)-(3).

$$\begin{bmatrix} i_{dw}^r \\ i_{qw}^r \end{bmatrix} = \begin{bmatrix} i_{ds}^r \\ i_{qs}^r \end{bmatrix} + \begin{bmatrix} i_{dn}^r \\ i_{qn}^r \end{bmatrix}, \quad (1)$$

$$\begin{bmatrix} i_{dn}^r \\ i_{qn}^r \end{bmatrix} = \begin{bmatrix} pC_s & -\omega_r C_s \\ \omega_r C_s & pC_s \end{bmatrix} \begin{bmatrix} v_{ds}^r \\ v_{qs}^r \end{bmatrix}, \quad (2)$$

$$\begin{bmatrix} v_{ds}^r \\ v_{qs}^r \end{bmatrix} = \begin{bmatrix} R_s + pL_{ds} & -\omega_r L_{qs} \\ \omega_r L_{ds} & R_s + pL_{qs} \end{bmatrix} \begin{bmatrix} i_{ds}^r \\ i_{qs}^r \end{bmatrix} + \begin{bmatrix} 0 \\ \omega_r \lambda_{PM} \end{bmatrix}, \quad (3)$$

where i_{dqw}^r : d and q axis output current of CSI, i_{dqs}^r : d and q axis stator current of PMSM, i_{dqn}^r : d and q axis current of filter capacitor, v_{dqs}^r : d and q axis voltage of filter capacitor, R_s : stator resistance of PMSM, L_{dqs} : d and q axis synchronous inductance of PMSM, ω_r : rotor angular speed of PMSM, λ_{PM} : flux linkage by permanent magnet and p : derivative operator. From those equations, the equivalent circuit can be derived as shown in Fig. 2, where $\lambda_{ds} = L_{ds}i_{ds}^r + \lambda_{PM}$ and $\lambda_{qs} = L_{qs}i_{qs}^r$.

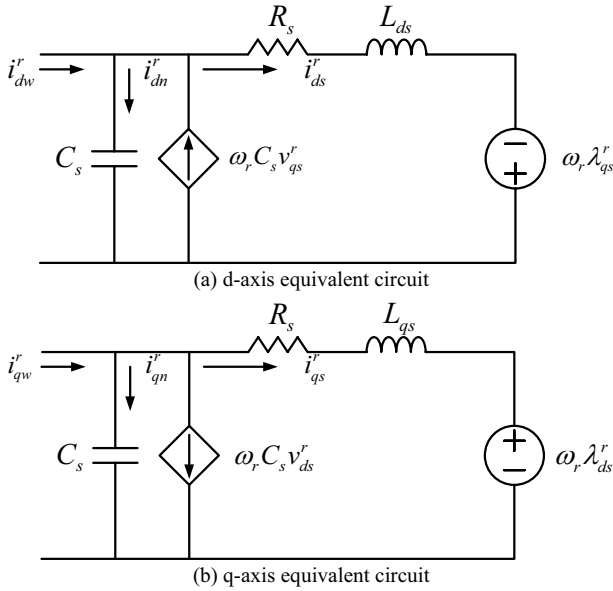


Fig. 2. Equivalent circuit of CSI including AC system and capacitor filter

III. CURRENT CONTROLLER DESIGN

The block diagram of model can be simply expressed as Fig. 3.

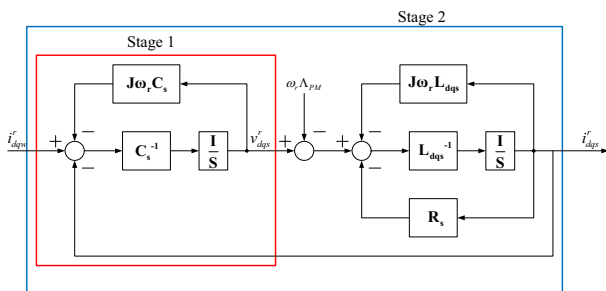


Fig. 3. Block diagram of two stage modeling

The current controller can be designed based on this block diagram. To control v_{dqs}^r in the first stage, simple P controller can be introduced where the coupling term is decoupled by feed-forward term. In the second stage, the PI controller can be proposed to control stator current of PMSM, i_{dqs}^r , where the coupling term can be decoupled by simple feed-forward term or the integrator with coupling error term which was already introduced as a complex vector current control concept [11].

A. Feed-forward decoupling method

The transfer function of the first stage can be set as the 1st order low pass filter with P controller. The output of the controller can be expressed by (4) where * stands for the reference and K_{pv} stands for the P gain.

$$\begin{bmatrix} i_{dw}^{r*} \\ i_{qw}^{r*} \end{bmatrix} = \begin{bmatrix} K_{pv} & 0 \\ 0 & K_{pv} \end{bmatrix} \begin{bmatrix} v_{ds}^{r*} - v_{ds}^r \\ v_{qs}^{r*} - v_{qs}^r \end{bmatrix} + \begin{bmatrix} i_{ds}^r \\ i_{qs}^r \end{bmatrix} + \begin{bmatrix} 0 & -\omega_r C_s \\ \omega_r C_s & 0 \end{bmatrix} \begin{bmatrix} v_{ds}^r \\ v_{qs}^r \end{bmatrix} = \begin{bmatrix} i_{ds}^r \\ i_{qs}^r \end{bmatrix} + \begin{bmatrix} sC_s & -\omega_r C_s \\ \omega_r C_s & sC_s \end{bmatrix} \begin{bmatrix} v_{ds}^r \\ v_{qs}^r \end{bmatrix}. \quad (4)$$

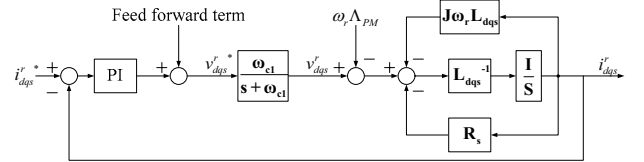


Fig. 4. Block diagram of 2nd stage controller design

If the feed-forward term is well matched to the real plant and it is assumed that the current reference is the same with the synthesizing current of CSI, then the transfer function in the first stage can be set as 1st order low pass filter where K_{pv} is $C_s \omega_{c1}$. As shown in Fig.4, and (5), if the feed-forward term is compensated with consideration of 1st order low pass filter, the transfer function of the 2nd stage can be expressed as 2nd order low pass filter.

$$\frac{\omega_{c1}}{s + \omega_{c1}} \begin{bmatrix} sK_{pd} + K_{id} & 0 \\ 0 & sK_{pq} + K_{iq} \end{bmatrix} \begin{bmatrix} i_{ds}^{r*} - i_{ds}^r \\ i_{qs}^{r*} - i_{qs}^r \end{bmatrix} = \begin{bmatrix} s(sL_{ds} + R_s) & 0 \\ 0 & s(sL_{qs} + R_s) \end{bmatrix} \begin{bmatrix} i_{ds}^r \\ i_{qs}^r \end{bmatrix}. \quad (5)$$

From above equation, if P gain (K_{pd} , K_{pq}) is set as $L_{ds} \omega_{c2}$, $L_{qs} \omega_{c2}$ respectively, and I gain (K_{id} , K_{iq}) is set as $R_s \omega_{c2}$ then the transfer function can be induced as (7) where the feed forward ($v_{dqs_ff}^r$) term is (6).

$$\begin{bmatrix} v_{ds_ff}^r \\ v_{qs_ff}^r \end{bmatrix} = \frac{s + \omega_{c1}}{\omega_{c1}} \left(\begin{bmatrix} 0 & -\omega_r L_{qs} \\ \omega_r L_{ds} & 0 \end{bmatrix} \begin{bmatrix} i_{ds}^r \\ i_{qs}^r \end{bmatrix} + \begin{bmatrix} 0 \\ \omega_r \lambda_{PM} \end{bmatrix} \right). \quad (6)$$

$$\begin{bmatrix} i_{ds}^r \\ i_{qs}^r \end{bmatrix} = \begin{bmatrix} \frac{\omega_{c1}\omega_{c2}}{s^2 + \omega_{c1}s + \omega_{c1}\omega_{c2}} & 0 \\ 0 & \frac{\omega_{c1}\omega_{c2}}{s^2 + \omega_{c1}s + \omega_{c1}\omega_{c2}} \end{bmatrix} \begin{bmatrix} i_{ds}^{r*} \\ i_{qs}^{r*} \end{bmatrix} \quad (7)$$

To calculate the feed-forward term, it seems to be required the differentiation. However, the derivative term can be calculated from the measured voltage and current using the parameters of PMSM. Although the derivative operator is not required to calculate feed-forward term, it has parameter dependency due to the open loop calculation using parameters of PMSM.

B. Decoupling method using complex current control concept

The design procedure is the same with above except feed-forward term. The equation (5) can be rewritten as (8).

$$\frac{\omega_{c1}}{s + \omega_{c1}} \begin{bmatrix} sK_{pd} + K_{id} & K_{idq} \\ K_{iqd} & sK_{pq} + K_{iq} \end{bmatrix} \begin{bmatrix} i_{ds}^{r*} - i_{ds}^r \\ i_{qs}^{r*} - i_{qs}^r \end{bmatrix} = \begin{bmatrix} s(L_{ds} + R_s) & -\omega_r L_q \\ \omega_r L_d & s(L_{qs} + R_s) \end{bmatrix} \begin{bmatrix} i_{ds}^r \\ i_{qs}^r \end{bmatrix} \quad (8)$$

If the coupled integrator gain (K_{idq} , K_{iqd}) is set as $-\omega_r L_{qs} \omega_{c2}$, $\omega_r L_{qs} \omega_{c2}$ respectively, then the transfer function is the same with (7). Additionally, if the mechanical time constant is large enough than electric time constant, the required feed-forward term is only back-EMF component as (9).

$$\begin{bmatrix} v_{ds_ff}^r \\ v_{qs_ff}^r \end{bmatrix} = \frac{s + \omega_{c1}}{\omega_{c1}} \begin{bmatrix} 0 \\ \omega_r \lambda_{PM} \end{bmatrix} = \begin{bmatrix} 0 \\ \omega_r \lambda_{PM} \end{bmatrix} \quad (9)$$

Like complex vector current controller, the pole of actual plant and zero of the current controller can be well canceled even if there are parameter errors.

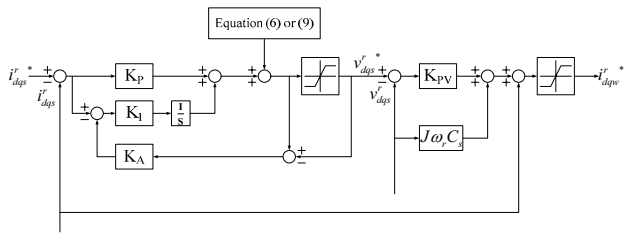


Fig. 5. Block diagram of designed multi-loop controller

C. Active damping method

To avoid instability of designed current controller due to the parameter error or other disturbances such as digital delay and nonlinearity of inverter, it is possible to embed virtual resistor which is already known as the active damping method.

In the proposed multi-loop current control scheme shown in Fig. 5, there are two possible locations of the virtual resistor in LC filter circuit in Fig.6. Series connection or parallel connection can be implemented in the designed current controller. As shown in Fig 7, the

virtual resistor (R_v) where is connected to the inductor in series (series active damping method) can be easily implemented with adding the feed-forward term which is set as $-R_v \frac{s + \omega_{c1}}{s} i_{dqs}^r$, and simple modification of the integrator gain (K_{id} , K_{iq}) which is set as $(R_s + R_v)\omega_{c2}$.

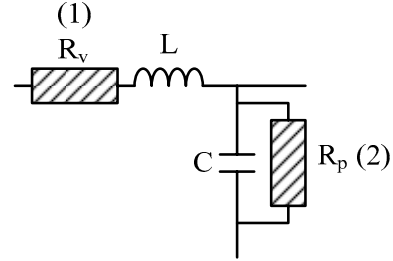


Fig. 6. Possible locations of virtual resistor

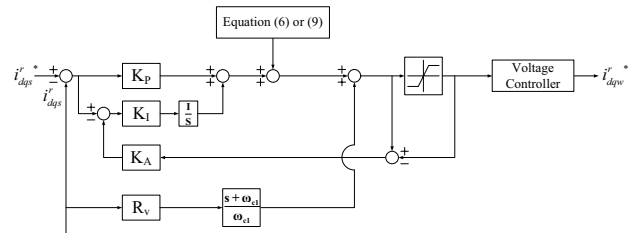


Fig. 7. Multi-loop current controller with the position (1) of virtual resistor in Fig. 6 (series active damping method)

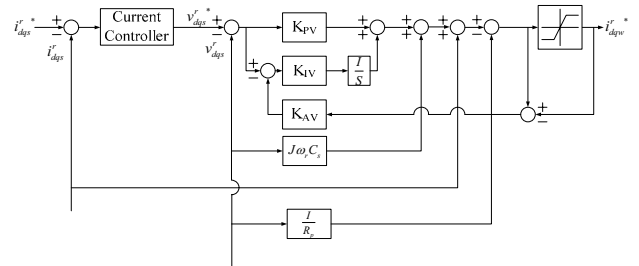


Fig. 8. Multi-loop current controller with the position (2) of virtual resistor in Fig. 6 (parallel active damping method)

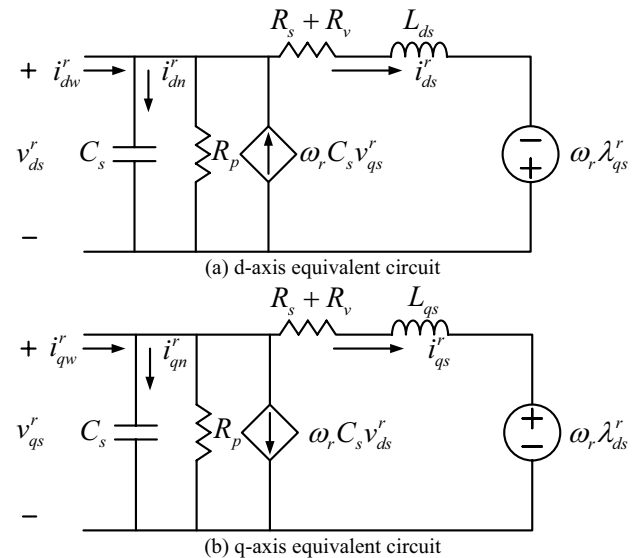


Fig. 9. Equivalent circuit of CSI including AC system and capacitor filter with virtual resistor

Fig. 8 shows the parallel active damping method

where the virtual resistor (R_p) is connected to the capacitor in parallel. In order to implement the parallel active damping method, the additional integrator is required in voltage control loop as well as the additional feed-forward term is necessary to express the virtual resistor which is connected to the capacitor in parallel.

The integrator gain, K_{iv} , can be set as $\frac{\omega_{cl}}{R_p}$, and the feed-

forward term for the parallel virtual resistor can be set as $-\frac{v_{dqs}^r}{R_p}$.

The equivalent circuit with virtual resistors can be described as Fig. 9.

IV. PWM STRATEGY

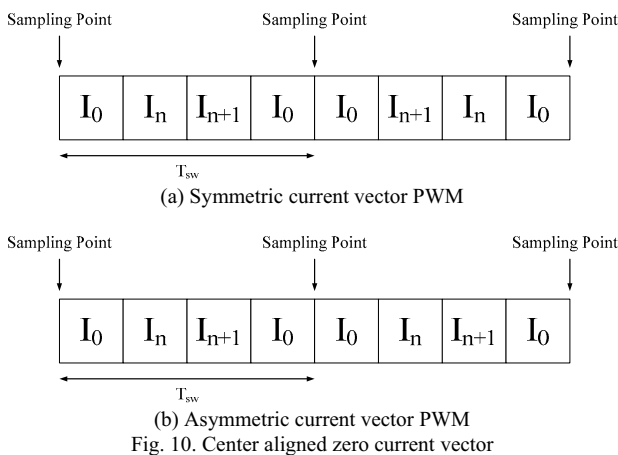


Fig. 10. Center aligned zero current vector

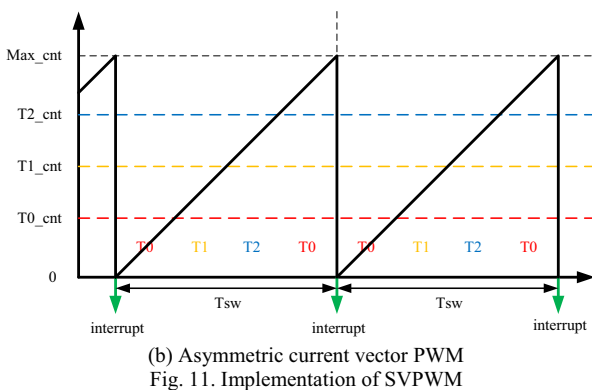
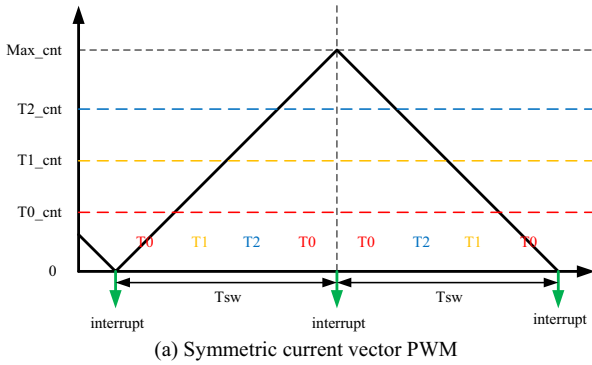


Fig. 11. Implementation of SVPWM

To generate gating signals, the space vector pulse width modulation (SVPWM) for CSI is adopted [12]. To achieve the proposed current control, measurement of the average voltage is important in a switching period with the switching frequency over 1 kHz. There are several options for the placement of zero current vectors in a switching period. To measure the average value of phase voltage in filter capacitor, the center aligned zero current vector placement has been used in this study.

There are two appropriate options for center aligned placement of zero current vector as shown in Fig. 10 (a) and (b), which are defined as symmetric PWM and asymmetric PWM, respectively. I_0 stands for the zero current vector, and I_n, I_{n+1} stand for the effective current vector.

Fig. 11 shows the implementation of SVPWM using FPGA logic which is described as Fig. 10. T_0, T_1 and T_2 stand for the dwell time of zero current vector and two effective current vectors, respectively.

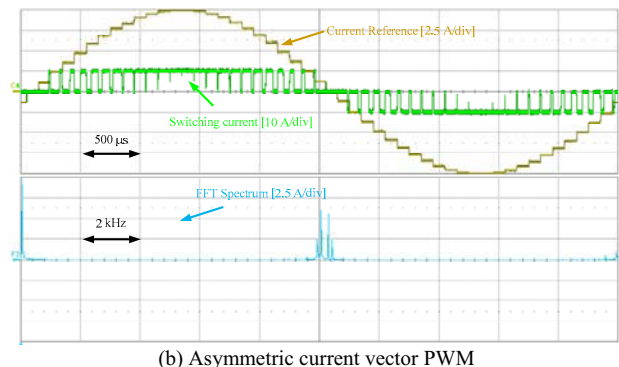
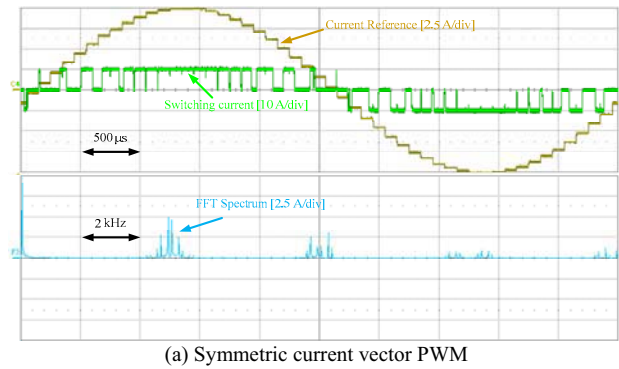


Fig. 12. PWM switching current and FFT results

Fig. 12 shows the switching currents waveform and their FFT results where modulation index is 1 with 10 kHz switching frequency. In the case of the symmetric PWM which is shown in Fig. 10 (a), there are other harmonic currents beside the switching frequency currents. It means that the designed LC filter might not attenuate this harmonic component due to limited cut-off frequency of LC filter. If the harmonic currents act as the disturbance to the proposed current controller, the controller cannot attenuate the disturbance because the frequency of the harmonics is over the band width of the controller. On the other hand, the asymmetric PWM which is shown in Fig. 10 (b), and there are little harmonic currents except on its own switching frequency.

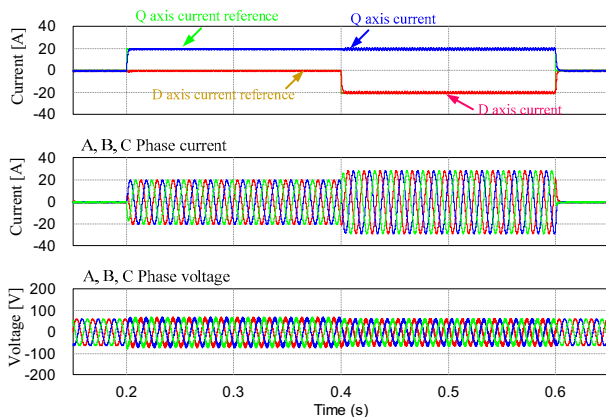
Although, the magnitude of switching frequency component currents is larger than that of symmetric PWM, the proposed current controller can regulate current if the cut-off frequency of LC filter is low enough to attenuate the switching component current. Thus, in this paper, the asymmetric PWM has been used for simulations and experiments.

V. SIMULATION RESULTS

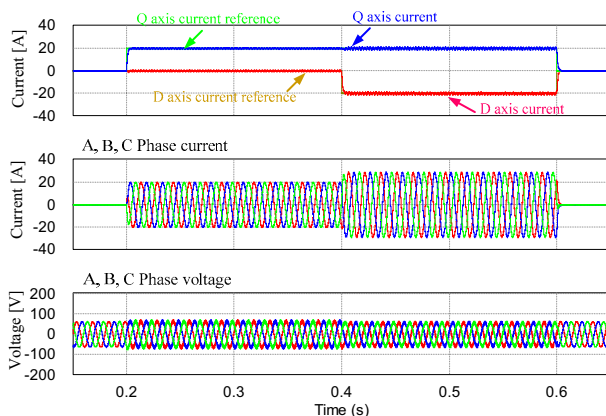
To evaluate the performance of the proposed multi-loop current controller, the computer simulation has been performed using PSIM® software. The parameters for simulation are listed on Table I.

TABLE I
PARAMETERS OF PMSM

Parameter	Values
Rated Power	11 kW
Rated Speed	1500 r/min
Pole	8
Back EMF constant	0.1478 V/(rad/s)
Synchronous d axis inductance	0.7 mH
Synchronous q axis inductance	0.7 mH
Stator resistance	40 mΩ
Delta connected filter capacitors	25 μF each
Switching frequency	10 kHz



(a) Feed-forward decoupling method



(b) Decoupling method with complex control concept

Fig. 13. Simulation results of proposed controller

The simulation has been performed with 1000 r/min of mechanical angular speed of rotor (electric angular frequency: 66.7 Hz) and 40 A of constant DC-link current.

In simulation, the virtual resistor, which is connected to the inductor in series, has been set as 20 times of the stator resistance to enhance the stability of the proposed current controller. In addition, the 2nd order low pass filter whose transfer function from reference current to real current is designed as (10).

$$\frac{\omega_n^2}{s^2 + 2\omega_n s + \omega_n^2}, \omega_n = 600\pi [\text{rad} / \text{s}] \quad (10)$$

If the parameter of the model is well matched to that of the actual plant, the results are almost same regardless of decoupling methods, as shown in Fig. 13.

VI. EXPERIMENTAL RESULTS

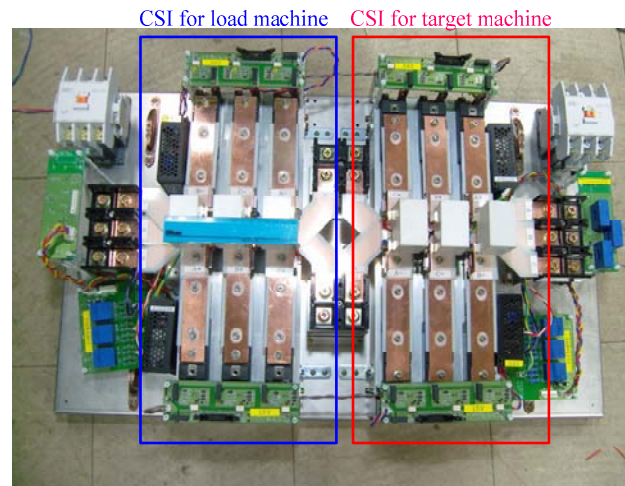


Fig. 14. CSI for experiment

Fig. 14 shows the fabricated prototype CSI for a laboratory experiment. The 1200V-75A level IGBT and diode has been used for the prototype CSI. The induction machine has been used as a load machine with the same current control method, and the PMSM, which has the same nominal parameters with PMSM for simulation, has been used as the machine under the test.

The parameters of the induction machine are listed on Table II.

TABLE II
PARAMETERS OF PMSM

Parameter	Values
Rated Power	11 kW
Rated Speed	1750 r/min
Pole	4
Stator resistance	69 mΩ
Rotor resistance	50 mΩ
Stator self inductance	14.1 mH
Rotor self inductance	14.1 mH
Mutual inductance	13.2 mH
Delta connected filter capacitor	25 μF

In the experiment, all of the condition is same with condition of the simulation where the mechanical angular speed of rotor : 1000 r/min, DC link current : 40 A, and 2nd order low pass filter : equation (10).

The experimental results were almost same regardless of decoupling methods due to the active damping control. Thus, in this paper, the experimental result with the

decoupling method using complex vector current control concept is shown.

In Fig. 15, the experimental results against step current reference changes are shown. The d and q axis current tracked the reference current well.

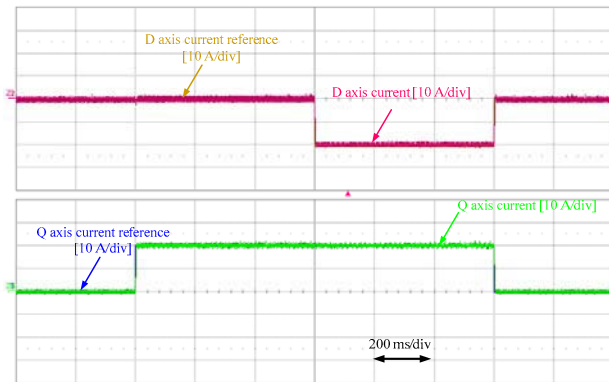
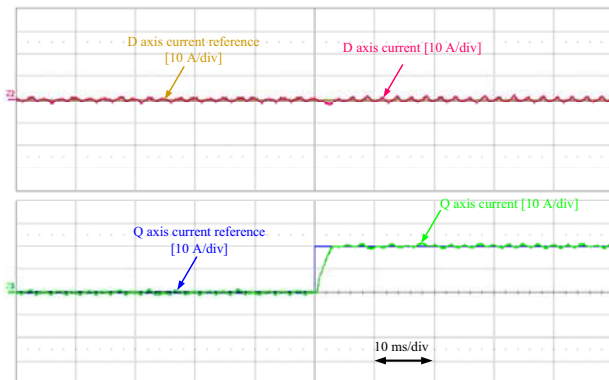
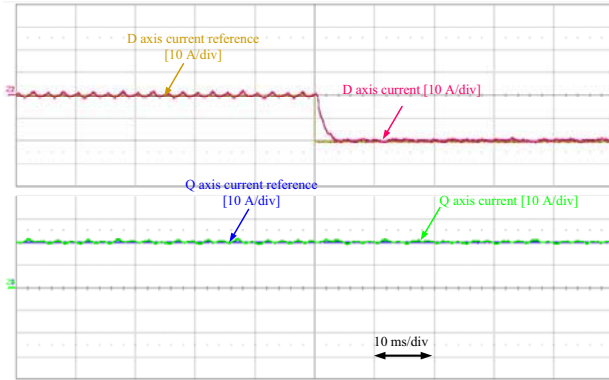


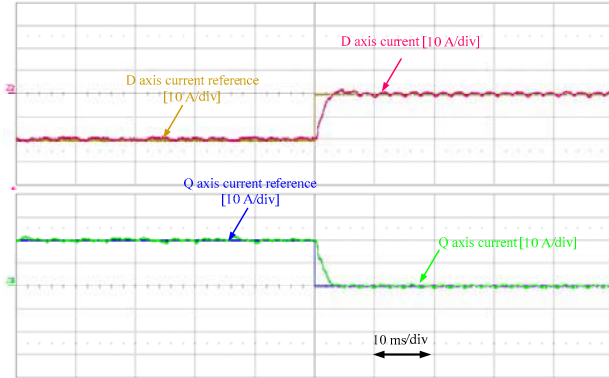
Fig. 15. Simulation results of proposed controller



(a) d axis current reference : 0 A, q axis current reference : 20 A



(b) d axis current reference : -20 A, q axis current reference : 20 A

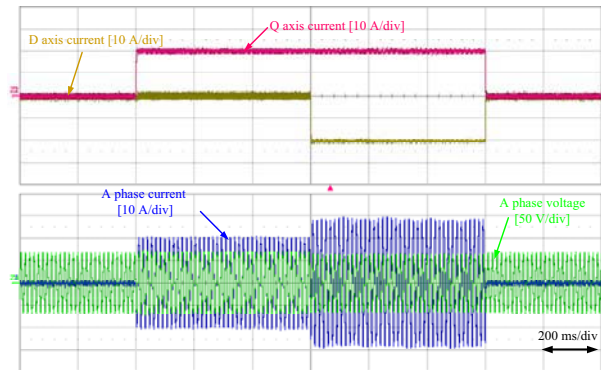


(c) d axis current reference : 0 A, q axis current reference : 0 A

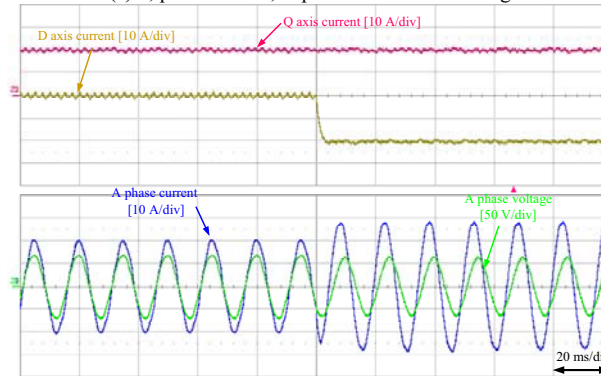
Fig. 16. Magnified view of Fig. 15

Because the damping ratio and natural frequency of 2nd order low pass filter are 1 and 300 Hz, respectively, the designed settling time is almost 3 ms.

As shown in Fig. 16 which is the magnified view of Fig. 15, the settling time of transient current with respect to step reference changes is almost 3 ms. Also, with the proposed decoupling method, there was little effect due to the coupling terms in the plant. Thus, it can be noted that the current controller has the designed characteristics.



(a) d,q axis current, A phase current and voltage



(b) d,q axis current, A phase current and voltage (magnified view)

Fig. 17. A phase current and voltage

Fig. 17 shows the A phase current and voltage. The waveform of the current and voltage is the almost sinusoidal form. As shown in Fig. 17 (b), the current has a little harmonic component. That harmonic current comes from the effect of distorted back EMF of PMSM, not the current controller itself.

VII. CONCLUSION

In this paper, the multi-loop current controller has been proposed for CSI-fed PMSM drive system to attenuate the resonance from LC filter. To design the multi-loop current controller, two-stage modeling has been employed. Additionally, two methods have been proposed to decouple the coupling term incurred by coordinate transformation to the synchronous reference frame. In addition, active damping methods based on virtual resistance has been embedded in the proposed controller to avoid the instability due to the parameter error and other disturbances such as digital delay and nonlinearity of an inverter. To measure the average value of phase voltage in filter capacitor, the center aligned

zero current vector placement has been used in this paper. Among the PWM method for center aligned zero vector, the asymmetric PWM method has been devised to minimize low frequency harmonic current. To validate the effectiveness of the proposed design scheme, the simulation and experimental result has been shown and discussed. The proposed current control method can be apply to not only PMSM, but also other AC system such as grid connection, induction machine by simply modifying gains and feed-forward terms.

REFERENCES

- [1] M. Salo, and H. Tuusa, "Vector-controlled PWM current-source-inverter-fed induction motor drive with a new stator current control method," *IEEE Trans. on Industrial Electronics*, vol. 52, no. 2, pp. 523-531, Apr. 2005.
- [2] S. A. Richter, B. Bader, and R.W. De Doncker, "Control of high power PWM current source rectifier," in *Proc. IPEC-2010*, pp. 1287-1292, Jun. 2010.
- [3] J. Dao, D. Xu, and Bin Wu, "A novel control scheme for current-source-converter-based PMSG wind energy conversion systems," *IEEE Trans. on Power Electronics*, vol. 24, no. 4, pp. 963-972, Apr. 2009.
- [4] Z. Wu, and G. J. Su, "High-performance permanent magnet machine drive for electric vehicle applications using a current source inverter," in *Proc. IECON 2008*, pp. 2812-2817, Nov. 2008.
- [5] H. Bilgin and M. Ermiş, "Design and implementation of a current-source converter for use in industry applications of D-STATCOM," *IEEE Trans. Power Electronics*, vol. 25, no. 8, pp. 1943-1957, Aug. 2010.
- [6] J. C. Wiseman, and Bin Wu, "Active damping control of a high-power PWM current-source rectifier for line-current THD reduction," *IEEE Trans. on Industrial Electronics*, vol. 52, no. 3, pp. 758-764, June 2005.
- [7] M. Salo, H. Tuusa, "A vector controlled current-source PWM rectifier with a novel current damping method," *IEEE Trans. on Power Electronics*, vol. 15, no. 3, pp. 464-470, May 2000.
- [8] Y. Nebu, "A simple method for suppression of resonance oscillation in PWM current source converter," *IEEE Trans. on Power Electronics*, vol. 20, no. 1, pp. 132-139, Jan. 2005.
- [9] Y. W. Li, B. Wu, N. R. Zargari, J. C. Wiseman, and D. Xu, "Damping of PWM current-source rectifier using a hybrid combination approach," *IEEE Trans. on Power Electronics*, vol. 22, no. 4, pp. 132-139, Jul. 2007.
- [10] P. C. Loh, and D. G. Holmes, "Analysis of multiloop control strategies for LC/CL/LCL-filtered voltage-source and current-source inverters," *IEEE Trans. on Industrial Applications*, vol. 41, no. 2, pp. 644-654, Mar/Apr. 2005.
- [11] F. Briz, M. W. Degner and R.D. Lorenz, "Analysis and design of current regulators using complex vectors," *IEEE Trans. Industrial Applications*, vol. 36, no. 3, pp. 817-825, May/June 2000.
- [12] Y. W. Li, B. Wu, D. Xu and N. R. Zargari, "Space vector sequence investigation and synchronization methods for active front-end rectifiers in high-power current-source drives," *IEEE Trans. Industrial Electronics*, vol. 55, no. 3, pp. 1022-1034, Mar. 2008.